

Controlled Growth of Y-Junction Nanotubes Using Ti-Doped Vapor Catalyst

N. Gothard,[†] C. Daraio,[‡] J. Gaillard,[†] R. Zidan,[§] S. Jin,[‡] and A. M. Rao^{*†}

Department of Physics and Astronomy, Clemson University, Clemson, South Carolina 29634, Department of Mechanical & Aerospace Engineering, University of California, San Diego, La Jolla, California 92093, and Savannah Research Technology Center, Aiken, South Carolina 29808

Received October 23, 2003

ABSTRACT

We demonstrate a bulk process for the synthesis of Y-junction carbon nanotubes using Ti-doped Fe catalysts. It is shown that the nanotube branching can be induced or stopped at will by tuning the Ti composition in the catalyst particle that seeds the growth of nanotubes. Detailed electron microscopic studies suggest that the mechanism for the observed Y-junction formation is mediated via catalyst particle attachment on the walls of a growing MWNT, from which the branching nanotubes nucleate and grow. By controlling the Ti concentration in the precursor, cascading Y-junction series as well as quadruple junctions have been successfully synthesized, offering the possibility for interesting device applications. The simplicity and controllability of such an in-situ Y-junction fabrication technique make it an excellent source of ready-made networks for potential nanoscale devices.

Semiconductor circuit technology has achieved great advances over the past few decades, mainly due to the continuing process of device miniaturization. A continued push in this direction is hampered by the high cost of miniaturization on the nanoscale, for instance, by expensive techniques such as electron beam lithography. Due to their unique electrical properties and inherent size, carbon nanotubes are being evaluated as next-generation circuit components.^{1,2} For example, two-contact electrical measurements across junctions between individual single-walled nanotubes (SWNTs) of different chiralities have demonstrated diode-like rectification behavior.¹ Further, fabrication of field effect transistors (FETs) in which a nanotube is used as the conduction channel is paving the way for the realization of nanotube-based electronics. Recently, theory has postulated that three-terminal “Y-junction” nanotubes should exhibit the gating behavior characteristic of transistors.³ Although clever means are being devised to manufacture such components en masse, they continue to present formidable challenges for large scale production.

Y-junction nanotubes have been prepared using alumina templates,⁴ by chemical vapor deposition (CVD) of products generated from a pyrolysis of metallocenes,^{5–7} and by nanowelding of overlapping isolated nanotubes using high-

intensity electron beams.⁸ These processes suffer either from the absence of controlled growth or the lack of ability to scale up for realistic applications. We report here a simple process for growing Y-junction nanotubes in bulk with the ability to control branching, a feature that shows tremendous promise for building nanoscale electronic networks.

It is widely known that aligned arrays of multiwalled nanotubes (MWNTs) can be readily grown on bare quartz or SiO₂/Si substrates by injecting a mixture of ferrocene (C₁₀H₁₀Fe) and xylene (C₈H₁₀) into a two-stage thermal CVD reactor consisting of a low temperature (~200 °C) preheater followed by a higher temperature main reactor.⁹ We have discovered that co-injection of a titanium-containing precursor such as C₁₆H₄₀N₄Ti, leads to the spontaneous growth of nanotube mats in which more than 90% of the tubes are branched to form multiwalled Y junctions. In our method, ferrocene is dissolved into a mixture of xylene and the titanium containing precursor C₁₆H₄₀N₄Ti at a concentration of 0.75 at. %. Mixtures with varying atomic concentration of Ti (0 to 3 at. %) are injected into the preheater maintained near 150 °C. The liquid mixture vaporizes in the preheater and is carried into the main quartz tube reactor, maintained at 750 °C, by a mixture of argon and hydrogen gases. Mats of oriented Y-junction nanotubes grow spontaneously on quartz substrates placed inside the reactor. Figure 1 shows an optical microscope dark field image of a Y-junction nanotube being pulled out of one such dense mat using a

* Corresponding author. E-mail: arao@clemson.edu

[†] Clemson University.

[‡] University of California.

[§] Savannah Research Technology Center.



Figure 1. Single Y-junction being separated from an array by applying a dc voltage between the array and a tungsten probe. Y-junction yield is greater than 90%.

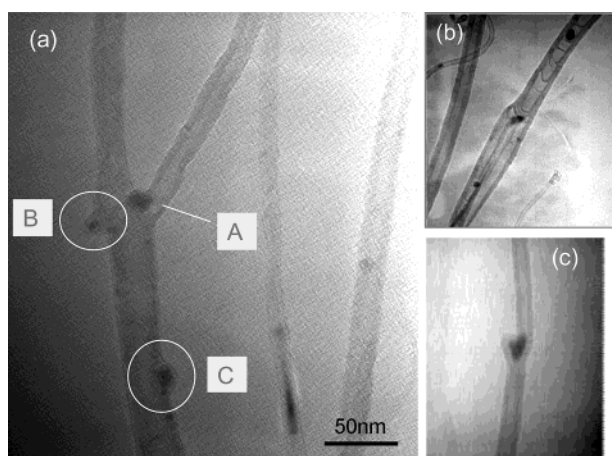


Figure 2. (a) TEM image of a Y-junction. An Fe-rich, Ti-doped catalyst particle is often present at the junction (marked A) leading to the formation of the two branches. Beginning of a secondary Y-junction is observed at B from catalyst particles that attach on the walls of the nanotube. A catalyst particle stuck to the sidewall of the stem (labeled C) does not induce branching, implying that a critical Ti concentration is needed in the particle to initiate branching. (b) Another example of a catalyst particle present at the junction. (c) A catalyst particle inducing Y-junction formation at an early stage.

sharpened W probe tip. A voltage of ~ 7 V was applied across the W probe tip and the Y-junction mat that was attached to the conducting SEM tape. More than 90% of the tubes present in the mat are Y-junction carbon nanotubes, suggesting that the addition of $C_{16}H_{40}N_4Ti$ promotes synthesis of Y-junction carbon nanotubes in bulk quantities.

Figure 2a is a transmission electron microscopy (TEM) photograph showing typical Y-junction morphology in a sample grown at 750 °C for 20 min. The MWNT structure of the base nanotube is visible. An Fe-rich catalyst particle with trace amounts of Ti is often present at the branching point of the Y-junction (marked A). Two additional sites where catalyst particles have attached onto the outer walls

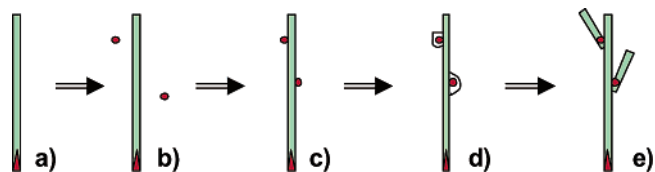


Figure 3. Sequence of events during the growth of a Y-junction: (a) nanotube nucleation and growth on substrate, (b) supply of Ti-containing Fe catalysts, (c) attachment of Fe–Ti catalyst particles on the sidewall of growing nanotubes, (d) nucleation of nanotube around the attached catalyst particle, and (e) growth of the Y-junction nanotube branches from the attached particles.

are labeled B and C, respectively. Growth of a branch in its initial stages is visible at B. Figure 2b is another example of catalyst particles present at the branching point, and Figure 2c shows the initiation of Y-junction growth from an attached particle.

EDS (energy dispersive X-ray spectroscopy) analysis of the catalyst particles at the junction during TEM studies indicates that the composition is predominantly Fe, with very small amounts of Ti present (less than a 1–2 at. %). This finding is consistent with the solubility of Ti in Fe at the operating conditions used in our experiment.¹⁰

Considering the fact that the Y-junction is not formed using the typical ferrocene-xylene mixture but is created only when the Fe catalyst is doped with Ti, we propose that Y-junction nucleation is initiated by the attachment of the Ti-containing Fe catalyst particle on the sidewall of the growing nanotubes, as demonstrated in the TEM micrographs of Figure 2. A sequence of events leading to the formation of Y-junction nanotubes is schematically illustrated in Figure 3. First, Ti-doped Fe catalyst particles seed nanotube nucleation and growth on the quartz substrate by the root growth method in which carbon is absorbed at the root and then ejected in the form of vertically aligned multiwall nanotubes (Figure 3a). As the supply of Ti-containing Fe catalyst particles continues (Figure 3b), some of the (Fe–Ti) particles attach onto the sidewalls of growing nanotubes (Figure 3c). Then, a nucleation of nanotube material around the attached catalyst particle occurs (Figure 3d), followed by growth of the Y-junction nanotubes from the attached particles (Figure 3e). This growth model is consistent with the TEM observations presented in Figure 2.

A consideration of the thermodynamic properties of the constituent materials helps explain why the Ti-doped Fe particles attach onto the growing nanotube wall. It is well-known that some elements in the periodic table have a stronger tendency for carbide formation than others. For example, Ti, Zr, Hf, Ta, Nb, and V are all strong carbide formers while Cr, Mo, and W, are moderate carbide formers. The heat of formation (ΔH_f) for TiC is $= -21.9$ Kcal/g-atom at 1000 K,¹¹ with the large negative value contributing to a decrease in overall free energy [$(\Delta G_f = \Delta H_f - T\Delta S)$ for TiC formation is -20.7 Kcal/g-atom] and leading to a strong driving force for the $Ti + C = TiC$ reaction. In contrast, the reaction and bonding of Fe and carbon is thermodynamically unfavorable since ΔH_f for the $3Fe + C = Fe_3C$ reaction is small and positive (+1.36 Kcal/g-atom

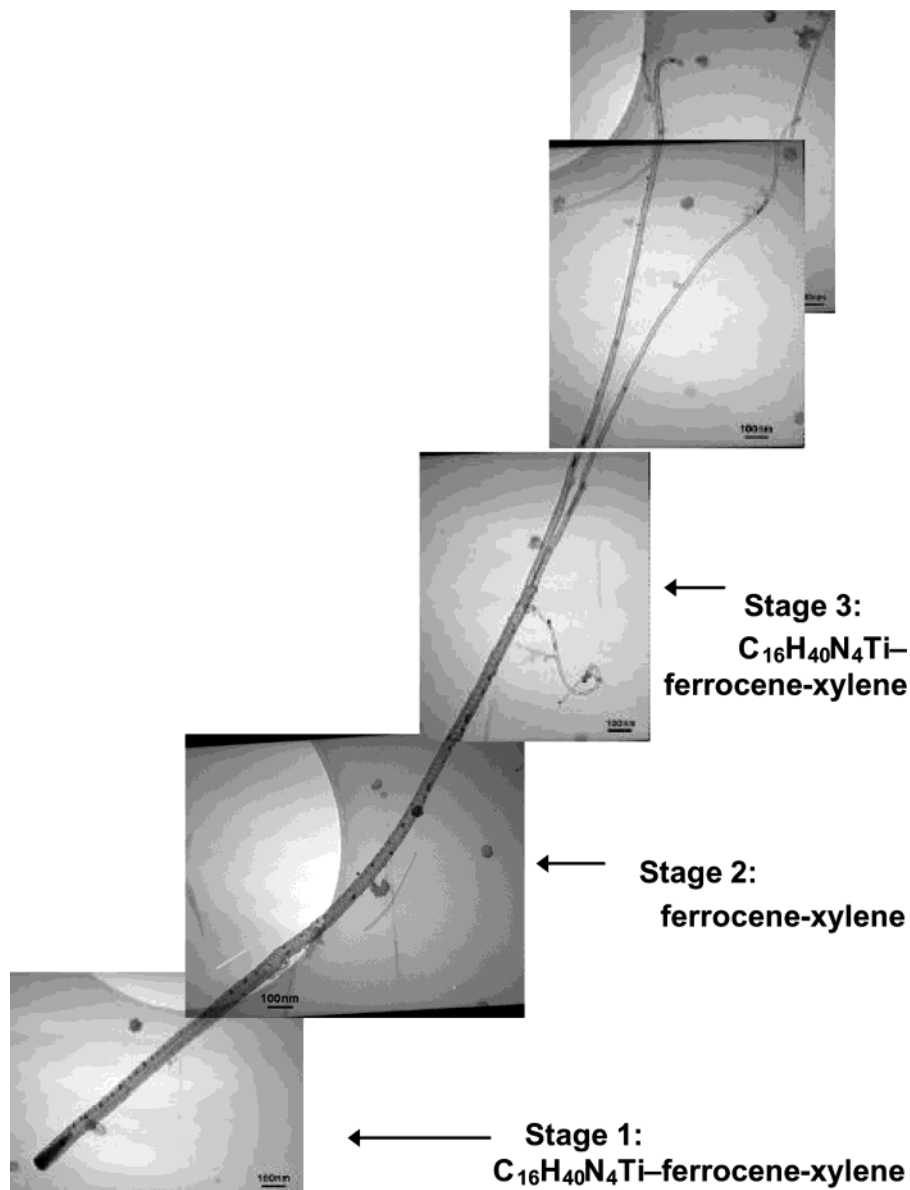


Figure 4. The absence of Ti during stage 2 (see text) inhibits branching, implying that the nanotube branching can be induced at will by controlling the catalyst composition. The scale bar indicated in each of the stacked images corresponds to 100 nm.

at 1000 K). The Fe–Ti catalyst particles would thus have a much stronger driving force for attaching to carbon nanotube walls than pure Fe catalyst particles, in agreement with the actual experimental observations. Besides Ti, inclusion of other strong carbide forming elements as dopants in the Fe catalyst should also facilitate the synthesis of Y-junction nanotubes. The ΔH_f values for some of the elements for the same operating temperature are ZrC (–23.4 Kcal/g-atom), HfC (–26), TaC (–17.6), NbC (–16.6), VC (–12.9), Cr_2C_3 (–4.9), Mo_2C (–3.5), and WC (–4.6).¹¹ Indeed, we have observed the formation of similar Y-junction nanotubes using both Hf- and Zr-doped Fe catalysts.

Figure 4 shows an example in which Y-junctions are formed at will using a three stage experimental procedure. Stage one consists of a 750 °C CVD run in which a $\text{C}_{16}\text{H}_{40}\text{N}_4\text{Ti}$ -ferrocene-xylene mixture is injected for 1–3 min, stage two of ferrocene-xylene injection for the next 30 min, and stage three of injection of the $\text{C}_{16}\text{H}_{40}\text{N}_4\text{Ti}$ -ferrocene-

xylene mixture for another 30 min. Due to the absence of Ti, no branching was induced during stage 2 of the injection process. In contrast, branching was induced during stage 3, as seen in Figure 4. Such capability to introduce Y-junctions at specific positions has the potential for synthesizing Y-junction nanotubes for future nanoelectronics applications. One possible approach for more precise placement of Y-junctions at specific locations along the length of the nanotubes is to introduce the $\text{C}_{16}\text{H}_{40}\text{N}_4\text{Ti}$ vapor simultaneously with a decrease in the carbon source (e.g., by limiting xylene) during CVD. Such an alteration would presumably halt nanotube formation while allowing the Ti-containing catalyst vapor to attach and nucleate the Y-junction seeds at essentially the same height on all the oriented nanotubes. Once the Ti–Fe catalyst seeds are attached, the supply of carbon can be resumed without the supply of catalyst vapor. This process can be repeated to produce an array of Y-junction nanotubes with one or more

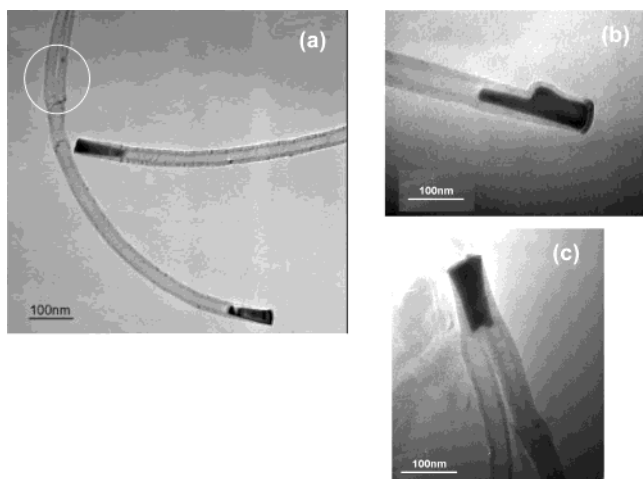


Figure 5. (a) TEM image showing the base-growth for the Y-junction nanotubes. The circle indicates the point of branching. Panels (b) and (c) represent occasional formation of V-junctions at the base caused by splitting of the catalyst particle.

branchings occurring at specific heights on the growing nanotubes.

Figure 5a is a TEM image which shows the presence of an initial catalyst particle at the bottom of the stem, supporting the base-growth model for nanotube formation, as depicted in Figure 3. These base particles remain stuck to the substrate, serving as sites for continued nanotube growth. Figures 5b and 5c show an occasional yet interesting formation of V-junctions at the base caused by splitting of the catalyst particle in higher temperature ($\sim 850^\circ\text{C}$) CVD runs. Continuous supply of the $\text{C}_{16}\text{H}_{40}\text{N}_4\text{Ti}$ vapor together with the ferrocene-xylene vapor often induces multiple branchings on the same nanotube. We have observed cascading Y-junction configurations as shown in Figures 6a and 6b. Such cascading Y-junctions could be useful as electrical signal splitters in nanotube-based circuits. A secondary Y-junction is also seen on the same nanotube in Figure 6b. Four-branched nanotubes of this sort could be useful as base structures for possible double-gated FET devices.

As expected, the growth of Y-junction nanotubes is sensitive to the CVD processing conditions of temperature, time, and catalyst concentration (Table 1). The at. % referred to in the table is the ratio of the number of moles of Ti or

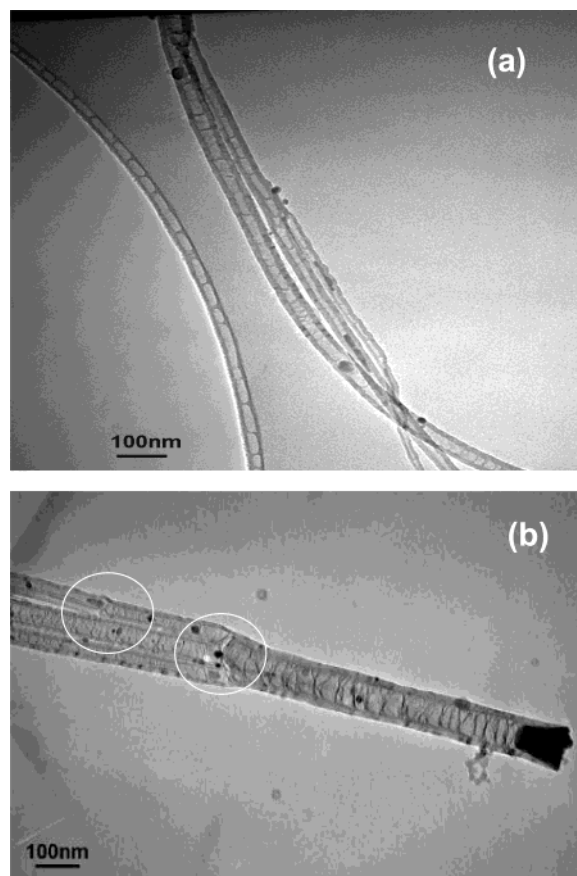


Figure 6. (a) Cascaded Y-junctions. (b) Another example of Y-junction cascade in which one of the three branches further splits into a secondary junction. The junctions are circled in the images.

Fe metallic atoms to the total number of moles of carbon in the solution. The optimal temperatures for Y-junction formation in a thermal CVD system appear to be in the $\sim 650\text{--}750^\circ\text{C}$ regime. The yield of Y-junction nanotubes gradually decreases with increasing CVD temperature, until between 800 and 850°C , Y-junctions rarely form. Instead, a small fraction of V-junction nanotube growth is favored at these temperatures (Figure 5c). The CVD runs were performed under $500\text{--}675$ sccm Ar and 75 sccm H_2 .

In summary, controlled branching of nanotubes has been demonstrated using a simple process of flowing a vapor catalyst consisting of Fe, Ti, and C. It is shown that nanotube branching can be induced at will via catalyst composition

Table 1. Effect of CVD Conditions on Yield of Y-Junction Nanotubes

at. % Ti/C	at. % Fe/C	CVD temp. ($^\circ\text{C}$)	injection duration (min.)	% of nanotubes with Y-junction	comments on morphology
3	0.7	650	20	~ 70	frequent double splitting
3	0.7	700–750	20–60	$\sim 75\text{--}100$	copious amounts of Y-junctions
3	0.7	800	20	$\sim 50\text{--}60$	irregular and corrugated stems
3	0.7	850	20	$\sim 10\text{--}15$	splitting occurs near base
1	0.7	750	30	25	corrugated stems, frequent double splitting

control. The Y-junction formation is initiated by catalyst particle attachment onto the side of growing MWNTs, from which the branching nanotubes grow. Cascading Y-junction series as well as quadruple junctions have been successfully synthesized, which may offer interesting device applications. The simplicity and controllability of such an in-situ Y-junction fabrication technique shows promise as a basis for potential nanoelectronics applications to ready-made nanoscale devices such as three-terminal nanoscale transistors, amplifiers, switches, and ballistic rectifiers.

Acknowledgment. This research was supported in part by the following grants: NSF NIRT 0304019, NSF 0132573, and NSF ERC EEC-9731680.

References

- (1) Avouris, Ph. *Acc. Chem. Res.* **2002**, *35*, 1026–1034.
- (2) Dekker, C. *Phys. Today* **1999**, *52*, 22–28.

- (3) Andriotis, A. N.; Menon, M.; Srivastava, D.; Chernozatonskii, L. *Phys. Rev. Lett.* **2001**, *87*, 066802–1–4.
- (4) Papadopoulos, C.; Rakitin, A.; Li, J.; Vedenev, A. S.; Xu, J. M. *Phys. Rev. Lett.* **2000**, *85*, 3476–3479.
- (5) Satishkumar, B. C.; John Thomas, P.; Govindaraj, A.; Rao, C. N. R. *Appl. Phys. Lett.* **2000**, *77*, 2530–2532.
- (6) Li, W. Z.; Wen, J. G.; Ren, Z. F. *Appl. Phys. Lett.* **2001**, *79*, 1879–1881.
- (7) Deepak, F. L.; Govindaraj, A.; Rao, C. N. R. *Chem. Phys. Lett.* **2001**, *345*, 5–10.
- (8) Terrones, M.; Banhart, F.; Grobert, N.; Charlier, J.-C.; Terrones, H.; Ajayan, P. M. *Phys. Rev. Lett.* **2002**, *89*, 075505–1–4.
- (9) Andrews, R.; Jacques, D.; Rao, A. M.; Derbyshire, F.; Qian, D.; Fan, X.; Dickey, E. C.; Chen, J. *Chem. Phys. Lett.* **1999**, *303*, 467–474.
- (10) *Metals Handbook*; Lyman, T., Ed.; American Society for Metals: Metals Park, Ohio, 1973; vol. 8, p 307.
- (11) *Selected Values of the Thermodynamic Properties of Binary Alloys*; Hultgren, R.; Desai, P.; Hawkins, D.; Gleiser, M.; Kelly, K., Eds.; American Society for Metals: Metals Park, Ohio, 1973; p 520.

NL0349294